ARTICLES

Precise determination of the void percolation threshold for two distributions of overlapping spheres

M. D. Rintoul

MS 1111, Sandia National Laboratories, P.O. Box 5800, Albuquerque, New Mexico 87185-1111

The void percolation threshold is calculated for a distribution of overlapping spheres with equal radii, and for a binary-sized distribution of overlapping spheres, where half of the spheres have radii twice as large as the other half. Using systems much larger than previous work, we determine a much more precise value for the percolation thresholds and correlation length exponent. The value of the percolation threshold for the monodisperse case is shown to be 0.0301 ± 0.0003, whereas the value for the bidisperse case is shown to be $p_c = 0.0287 \pm 0.0005$. The fact that these are significantly different is in contrast with previous, less precise works that speculated that the threshold might be universal with respect to sphere size distribution.

I. INTRODUCTION

The concept of percolation was originally introduced to describe the flow of a fluid through a porous medium [1]. However, once an understanding regarding the universality of the problem was achieved, much of the mathematical work was relegated to lattice models that showed the same mathematical behavior with regard to the critical exponents [2–7]. While work on lattice percolation allowed for ease of simulation and mathematical tractability in special cases, this technique also lost some of the information regarding quantities such as pore size and flow rate.

Continuum percolation differs from lattice percolation in the sense that the problem is not restricted to a lattice, but is defined on the full D-dimensional space. There are two common continuum percolation problems based on overlapping spheres. The first is that of percolation of overlapping disks or spheres themselves [8–16]. This problem is analogous to the lattice percolation problem where the points are distributed randomly through space. A bond between two sites is formed when the distance between the two spheres is less than the sum of the two sphere radii (i.e., the two spheres overlap). This is what is usually referred to in the literature under the name of *continuum percolation*. A variation of this includes percolation of partially overlapping spheres with hard, nonoverlapping cores (the cherrypit model) [17]. In the limit that the overlapping part disappears, one is left with the problem of percolation of hard spheres. This is generally considered identical to the determination of the random close packing limit.

The other type of continuum percolation problem is the complementary problem to the first type. In this case, one considers a system of overlapping spheres and asks when the space not occupied by the spheres percolates [18–20]. This is generally referred to as *void percolation*, but is also referred to as *Swiss-cheese percolation* (although *complementary continuum percolation* would probably be a more descriptive term). This type of percolation is very similar to the

original definition involving fluid flow through a porous media.

Without any additional mathematical tools to help solve the problem, the question of determining whether or not there is a connected path for fluid to flow through a system of overlapping spheres would be difficult. Fortunately, Kerstein [18] showed that the problem could be mapped to the bond percolation problem on the edges of the Voronoi tessellation of the sphere centers. The primary computational problem is then reduced to that of determining the Voronoi tessellation [21]. Once the bond percolation model is established from that, one can apply well-known Monte Carlo techniques to determine the percolation threshold and related exponents.

Due to the increased complexity involved in calculating the Voronoi tessellation and the increased memory required to store the corresponding data structures, the size of the problem that one can effectively work on is greatly reduced relative to lattice or standard continuum percolation problems. The net effect is that there has been much less work done on the void problem, and the numerical results that have been obtained are much less precise. One interesting recent result has shown that the void percolation threshold for a binary system of spheres with unequal radii seems to be equivalent to that of a system of spheres with equal radii [20].

The fact that the void percolation thresholds for two systems with different sphere distributions should be the same would be a remarkable result if it were true, since the arguments that apply to universality of the critical exponents should not apply to the percolation thresholds. There has been much more work done on the question of percolation threshold universality for the problem of the space occupied by the spheres. Theoretical works indicate that such a universality should not exist [22,23], and computational studies of simple systems have borne out these results [14].

In this paper, we use much larger systems to obtain a precise value for the void percolation threshold for a system

of equisized spheres. In a similar way, we calculate the void percolation threshold for a set of spheres that have two different values for their radii, and show it is statistically different. We also calculate the correlation length exponent ν, and confirm that it is similar to that of lattice percolation and ordinary continuum percolation, as universality dictates.

In Sec. II, we give the mathematical background for the calculations of the correlation length exponent, along with the formulas used to calculate the percolation threshold p_c. Section III gives a detailed explanation of the algorithms used to construct the Voronoi tessellation associated with the spheres. The numerical details of the calculation are given in Sec. IV. The results of the calculation are given in Sec. V and compared with previous results. Finally, we summarize our conclusions in Sec. VI.

II. MATHEMATICAL BACKGROUND

A. Scaling laws

The precise value of the percolation threshold p_c for any system is defined in the limit of a system of infinite size. In practice, one can only calculate the value of the effective percolation threshold for a system of finite linear size L, $p_c(L)$. Then, one uses the scaling relation [3]

$$p_c(L) - p_c \propto L^{-1/\nu}, \tag{1}$$

where ν is the correlation length exponent.

In many lattice applications, it is a natural variable to write the scaling relation in terms of the variable L. However, in continuum systems, especially those with a variety of particle sizes, the number of particles N is a much more natural scaling variable. Using the fact that

$$N \propto L^D, \tag{2}$$

where D is the dimensionality of the embedding space, we can write Eq. (1) as

$$p_c(N) - p_c \propto N^{-1/(\nu D)}. \tag{3}$$

In order to calculate p_c, one must calculate $p_c(N)$ for different values of N, and plot them against $N^{-1/(\nu D)}$. For large values of N, this should be linear, and an extrapolation of the line to the limit $N^{-1/(\nu D)} \to 0$ $(N \to \infty)$ will give the result for the infinite system.

Before that calculation can be done, one also needs the value of ν. Values obtained for lattice models can be used, but for the sake of self-consistency, we will calculate ν from the data. This is done by calculating $p_c(N)$ for a large number of finite systems of N particles, and calculating the standard deviation $\Delta p_c(N)$ of those values. Then, one applies the scaling relation [3]

$$\Delta p_c(N) \propto N^{-1/(\nu D)} \tag{4}$$

to calculate ν.

There is another reason to independently calculate ν in the case of the void problem. It turns out that universality does *not* apply to all exponents in this case. The mechanical and transport exponents are different, due to the narrow bottlenecks that form in the system [24]. It is generally understood that ν does not change in this case, but there have

not been any calculations of ν for void percolation systems that could confirm this with precision.

B. Voronoi diagrams

A Voronoi diagram of a set of points is a decomposition of the space into regions (which we will call *cells*) that are associated with each point, such that every point in the Voronoi cell is closer to the associated point than any other point in the system [25]. Mathematically, if there are N sphere centers, and the coordinates of the sphere centers are given by $\mathbf{x}_i$, where $i = 1, \ldots, N$, then the Voronoi cell associated with i is defined as the set of all points $\mathbf{x}$ such that

$$d(\mathbf{x}, \mathbf{x}_i) < d(\mathbf{x}, \mathbf{x}_j), \quad \forall i \neq j. \tag{5}$$

In this definition, $d(\mathbf{x}, \mathbf{y})$ is the distance between points $\mathbf{x}$ and $\mathbf{y}$.

The boundaries of the Voronoi cells represent points that are equidistant from two or more sphere centers. From this, it is easy to see physically that any void space in the system, if it exists, can be associated with a Voronoi vertex since the Voronoi vertices represent points in the systems that are as far away as possible from its associated sphere centers (generally four, for random three-dimensional systems). In the same way, any connected path in the void region can be associated with a Voronoi edge that links two Voronoi vertices. The edge represents the set of points equidistant to the sphere centers that are common to the two vertices that it connects. Therefore, once the network of vertices and edges has been established, it is just necessary to determine which of the vertices represent void space and which of the edges are not intersected by any spheres. This procedure is proven by Kerstein [18].

The method of solving the void percolation problem for overlapping spheres with possibly different radii follows the same basic idea, but uses a more general version of the Voronoi tessellation known as a *radical Voronoi tessellation* [26]. This definition is similar to the definition for the standard Voronoi tessellation, except now for a sphere i with center at $\mathbf{x}_i$, there is an associated radius r_i, and the definition of the radical Voronoi cell becomes the set of points $\mathbf{x}$ such that

$$d(\mathbf{x}, \mathbf{x}_i)^2 - r_i^2 < d(\mathbf{x}, \mathbf{x}_j)^2 - r_j^2, \quad \forall i \neq j. \tag{6}$$

This is known as a ''radical'' Voronoi tessellation since the cell boundaries now represent points that are equidistant from tangent lines drawn from each sphere. This definition is often referred to as a *power diagram* in the mathematics literature [27].

This tessellation has a number of nice properties, including preserving planarity of the faces that separate the resulting cells. Most importantly, the vertices and edges contain precisely the same connectivity information as the case of equisized spheres [20], so the algorithm is essentially unchanged. In the case of all sphere radii being equal, the standard Voronoi tessellation is recovered.

III. VORONOI DIAGRAM CONSTRUCTION

The fact that the passages through the void space can be mapped to the edges in a Voronoi tessellation is indeed a

fortuitous one, since the problem is very difficult to solve without prior knowledge of this fact. However, this is still one of the more time-consuming steps in the calculation, and having an efficient method of constructing the Voronoi tessellation is important.

There are a number of ways to create Voronoi tessellations used in this simulation, depending on how the points are arranged, the specific information needed from the tessellation, and what boundary conditions are used. Early works were based on identifying the vertices first by searching through a collection of nearby sphere centers and checking each combination of four different sphere centers to see if it had a corresponding Voronoi vertex [28]. Other early methods included identification of the Voronoi faces first by constructing the planes associated with the neighboring points and then identifying the vertices [29]. This method is especially useful if one is interested in the details of a small number of cells.

There were two methods of calculating the Voronoi tessellation, both different than the two described above. The primary method was via insertion. To use this method, one starts with an initial tessellation, and then inserts the new sphere center and changes the structure accordingly [21]. This method is very quick since it can be implemented by finding a single vertex that will be affected by the insertion, and recursively searching through all of its neighbors until one has identified all of the vertices that will be affected. Determining whether or not a vertex will be affected is just a matter of checking to see whether it is closer to the new sphere center than it is to its previous sphere centers (taking into account the radii in the case of the radical tessellation). Because searches just involve looking at neighbors of vertices currently being considered, there is no need to search for neighbors using geometrical comparisons.

The primary drawback with the method is that one needs some initial tessellation to start using the method. This was accomplished by starting with a small initial set of particle centers and performing a ''shooting''-type tessellation. For this tessellation, a single vertex was initially located, and then its neighboring vertices were then located. The determination of neighboring vertices is fairly straightforward in this case, as one knows that the neighboring vertices will have three of the four particle centers in common. Using this information it is simple enough to search along the equidistant line of these three centers to find the position of the neighboring vertex. This is a little slower than the previous method since there are more geometrical calculations to perform. Also, the data structures needed to perform all of the operations efficiently are much more complex in this method, due to the fact that one must associate a newly found vertex with all of its neighbors that may have already been found.

The amount of time for the insertion algorithm to perform N insertions generally behaves as $O(N)$ for N particles, assuming them to be uniformly distributed. It has a worst case behavior of $O(N^2)$ in the case of certain pathological distributions of particles, but those distributions were not relevant for these simulations. The shooting algorithm had a slightly worse than $O(N)$ scaling, but its behavior was not studied in detail since it was only used on small sets of particles and never played a significant role in the amount of time taken to do the calculations.

IV. NUMERICAL DETAILS

To answer the question regarding universality of the percolation threshold for different sphere size distributions, we chose to study two different systems. In both sets, half of the spheres had a radius of r_1, and the other half were assigned a radius of r_2. In the first set, $r_1 = r_2$, while in the second, $r_1 = r_2/2$. The factor of 2 in radii sizes was chosen with the hope that if there were differences in the percolation threshold, it would manifest itself strongly at that ratio. This was not based on any analytical prediction, but simply on the fact that in the limit that r_1/r_2 approaches either 0 or 1, one recovers the equisized case. Given limited resources to try many different values of r_1/r_2, one would hope that $r_1/r_2 = 1/2$ would be a possible candidate for a measurable difference in the percolation threshold.

Finite-size scaling was used to calculate ν and p_c, as dictated by Eqs. (3) and (4). Values of N ranged from 312 to 80 000, with the value increasing by approximately a factor of 2 each time. The number of configurations used to generate the data for each value of N ranged from 10 000 for $N = 312$ to 500 for $N = 80 000$.

Calculation of the percolation threshold for each system was done by a binary search through the different values of volume fraction for a fixed set of sphere positions and sphere radii ratios. One started with an initial value for the upper and lower bound for the percolation threshold for the system, and chose a first test value halfway between the two for an initial guess. If the void percolated, the upper bound was set at this value, and a new guess was chosen halfway between the lower bound and the new upper bound. Similarly, if the void did not percolate, the lower bound was set at this value and a new value was chosen halfway between the new lower bound and the upper bound. The search was reiterated until the difference between two previous guesses was less than a specified tolerance. This tolerance was chosen to be 10^{-6}. Periodic boundary conditions were employed, and percolation was defined as the point when the largest cluster spanned one of the directions of the unit cell and overlapped with itself.

The sphere radii were determined using the fact that in a system of overlapping spheres that are randomly distributed over a periodic unit cube, the average total void volume fraction is given by e^{η}, where η is defined by

$$\eta = \sum_{i=1}^{N} \frac{4}{3} \pi r_i^3 \qquad (7)$$

and is just the sum of all of the individual sphere volumes. It should be noted that this is not the precise value of the total volume in each system, but it is very close. Attempts were made to measure the effect of this by calculating the exact volume in the system in systems with small N, and adjusting the radii until such a specific volume was reached, but this had no measurable effect on the results.

The vertex percolation method was used to determine the Voronoi vertex network for the first 500 sphere centers (or all of them for the $N = 312$ case), and then the insertion method was used for the rest of the centers for each sample.
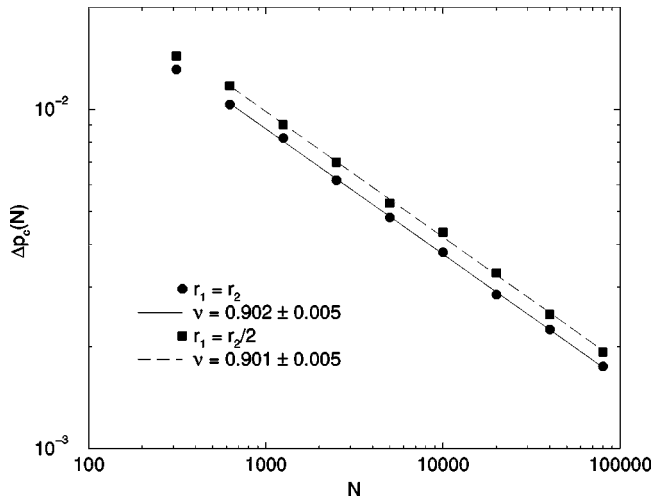
FIG. 1. Log-log plot of the standard deviation $\Delta p_c(N)$ as a function of N for the case of $r_1 = r_2$ (filled circles) and $r_1 = r_2/2$ (filled squares). The lines represent a least-squares power-law fit to the data. The case $N = 312$ is excluded from the fit since it appears to be out of the scaling regime.

FIG. 2. Plot of $p_c(N)$ vs $N^{1/(\nu D)}$. The solid line represents a linear fit to the $r_1 = r_2$ data for $N \lesssim 2500$, while the dashed line represents the same thing for the $r_1 = r_2/2$ case. The y intercepts for the two fits are very clearly different.

It should be noted that in the case where all of the sphere radii are the same size, the Voronoi network does not change as the sphere radii change, and it only needs to be calculated once. However, in the case where the radii are different, the vertex network needs to be recalculated for each value of p. The main effect of this is that the cases where $r_1/r_2 = 1/2$ took significantly longer to run.

V. RESULTS AND DISCUSSION

The log-log plot of $\Delta p_c(N)$ vs N is shown in Fig. 1. Although the numerical values of $\Delta p_c(N)$ are different for each of the two cases, the slope values are indistinguishable within the numerical tolerance of the simulation. The value for $N = 312$ is not used for the fit, as it appears to lie outside the scaling region. The slope of the line for the $r_1/r_2 = 1$ case corresponds to a value of $\nu = 0.902 \pm 0.005$, while the $r_1/r_2 = 1/2$ case gives a value of $\nu = 0.901 \pm 0.005$.

This value is significantly larger than the value of 0.84 computed for void percolation from two different sphere distributions (one equisized, one not) in [20]. However, that work used only five different values of N that ranged from 100 to 10 000 for the equisized case, and used only four values (ranging from 100 to 3162) for the nonequisized case. As demonstrated here, much of that region did not seem to lie in the scaling regime. Also, fewer samples were used for each value of N. The value of ν calculated here is much more in line with the value 0.88 reported for lattice calculations [3], and the value 0.89 ± 0.01 reported for ordinary continuum percolation [16]. It should be noted that the value of 0.84 given in [20] is not completely out of line, given the errors for the different cases. We also note here that for this and later comparisons with [20], that their nonequisized case had a different value of $r_1/r_2 = 1/4$, and the number fraction
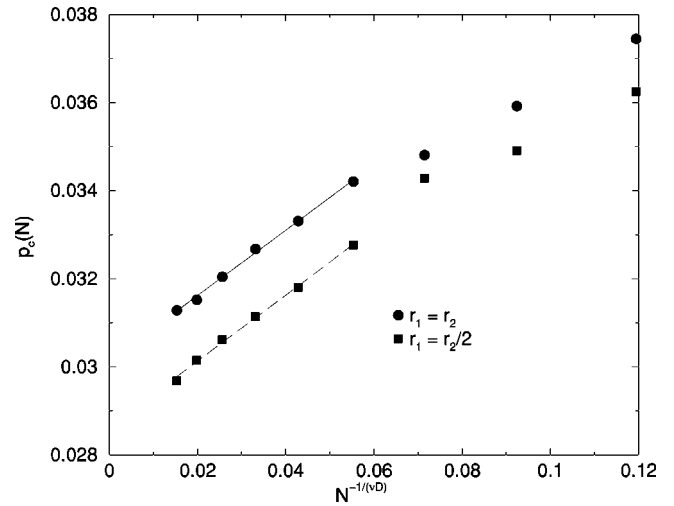
of larger spheres was 0.2070 (instead of 1/2 for the current study).

Using a value of $1/(\nu D) = 0.37$ (corresponding to $\nu = 0.901$), the values of $p_c(N)$ were plotted against $N^{-1/(\nu D)}$. Then a least-squares fit was done to fit a line through the values for $N \geq 2500$ to extrapolate the value of the void percolation threshold for $N^{-1/(\nu D)} = 0$ ($N = \infty$). These data are shown in Fig. 2. From the plots, it is very clear that the values are significantly different. For $r_1/r_2 = 1$, we find that $p_c = 0.0301 \pm 0.0003$, while for $r_1/r_2 = 2$ the value is $p_c = 0.0287 \pm 0.0005$. Not only are the values significantly different but from the graph it is clear that the extrapolation to $N = \infty$ will give different values. These values are very similar to the values given in [20], but are much more precise, allowing the difference between the two values to be seen clearly.

VI. CONCLUSIONS

We have precisely calculated the void percolation threshold for two distinct overlapping sphere systems. First, as a benchmark, we have calculated a much more precise value of the void percolation threshold for a system of equisized spheres. Then we have shown a recent conjecture that this value might be universal for different sphere size distributions to be false by calculating the void percolation threshold for a set of spheres with half of the spheres having radii twice as large as the others.

ACKNOWLEDGMENTS

[1] S. R. Broadbent and J. M. Hammersly, Proc. Cambridge Philos. Soc. **53**, 629 (1957).

[2] M. F. Sykes and M. Glen, J. Phys. A **9**, 87 (1976).

[3] D. Stauffer and A. Aharony, *Introduction to Percolation Theory*, 2nd ed. (Taylor & Francis, Bristol, 1992).

[4] P. Grassberger, J. Phys. A **25**, 5867 (1992).

[5] M. D. Rintoul and H. Nakanishi, J. Phys. A **25**, L945 (1992).

[6] R. M. Ziff, Phys. Rev. Lett. **69**, 2670 (1992).

[7] M. D. Rintoul and H. Nakanishi, J. Phys. A **27**, 5445 (1994).

[8] S. W. Haan and R. Zwanzig, J. Phys. A **10**, 1547 (1977).

[9] E. T. Gawlinski and H. E. Stanley, J. Phys. A **14**, L291 (1981).

[10] G. Stell, J. Phys. A **17**, L855 (1984).

[11] I. Balberg and N. Binenbaum, Phys. Rev. A **31**, 1222 (1985).

[12] I. Balberg, Phys. Rev. B **37**, 2391 (1988).

[13] S. B. Lee, Phys. Rev. B **42**, 4877 (1990).

[14] B. Lorenz, I. Orgzall, and H.-O. Heuer, J. Phys. A **26**, 4710 (1993).

[15] A. Okazaki, K. Maruyama, K. Okumura, Y. Hasegawa, and S. Miyazima, Phys. Rev. E **54**, 3389 (1996).

[16] M. D. Rintoul and S. Torquato, J. Phys. A **30**, L585 (1997).

[17] S. B. Lee and S. Torquato, Phys. Rev. A **41**, 5338 (1990).

[18] A. R. Kerstein, J. Phys. A **16**, 3071 (1983).

[19] S. Feng, B. I. Halperin, and P. N. Sen, Phys. Rev. B **35**, 197 (1987).

[20] S. C. van der Marck, Phys. Rev. Lett. **77**, 1785 (1996).

[21] F. Aurenhammer, ACM Comput. Surv. **23**, 345 (1991).

[22] I. Balberg, Philos. Mag. B **6**, 991 (1987).

[23] R. Meester, R. Roy, and A. Sarkar, J. Stat. Phys. **75**, 123 (1994).

[24] B. I. Halperin, S. Feng, and P. N. Sen, Phys. Rev. Lett. **54**, 2391 (1985).

[25] A. Okabe, B. Boots, and K. Sugihara, *Spatial Tessellations: Concepts and Applications of Voronoi Diagrams* (Wiley, New York, 1992).

[26] B. J. Gellatly and J. L. Finney, J. Non-Cryst. Solids **50**, 313 (1982).

[27] F. Aurenhammer, SIAM J. Comput. **16**, 78 (1987).

[28] J. L. Finney, J. Comput. Phys. **32**, 137 (1979).

[29] W. Brostow and J.-P. Dussault, J. Comput. Phys. **29**, 81 (1978).